symmetry

MDPI

Article

New Features in the Differential Cross Sections Measured at the LHC

Oleg Selyugin

Bogoliubov Laboratory of Theoretical Physics, Joint Institute for Nuclear Research, 141980 Dubna, Russia; selugin@theor.jinr.ru

Abstract: The critical analysis of the new experimental data obtained by the ATLAS Collaboration group at 13 TeV is presented and the problem of the tension between data of the ATLAS and TOTEM Collaborations is considered. The analysis of new effects discovered on the basis of experimental data at 13 TeV MDPI: ref is not allowed in abstract, please correct. and associated with the specific properties of the hadron potential at large distances is carried out taking account of all sets of experimental data on elastic proton-proton scattering obtained by the TOTEM and ATLAS Collaborations in a wide momentum transfer region. It also gives quantitative descriptions of all examined experimental data with a minimum of fitting parameters. It is shown that the new features determined at a high statistical level give an important contribution to the differential cross sections and allow the research analytic properties and symmetries into hadron interactions at large distances.

Keywords: hadron; elastic scattering; high energy; generalazed parton structure

check for updates

Citation: Selyugin, O. New Features in the Differential Cross Sections Measured at the LHC. *Symmetry* **2023**, *15*, 760. https://doi.org/10.3390/sym15030760

Academic Editor: Vitaly Beylin

Received: 12 February 2023
Revised: 6 March 2023
Accepted: 14 March 2023
Published: 20 March 2023

1. Introduction

Proton is one of the most important object in Universe. Its structure and interaction are related with fundamental laws and symmetries. It is concern especially analytic connections the hadron interactions at low and super high energy. For example, the search for the effects of T-invariance violation [1] (which, under the condition of CPT symmetry, is equivivalent to CP violation) is carried out in order to find an explanation for the observed baryon asymmetry of the Universe, the magnitude of which is underestimated within the Standard Model (SM) by several orders of magnitude [2]. To get hard predictions for hadronic interactions at ultrahigh and low energies, we need to know with the highest possible accuracy the structure of hadrons and their interactions. The main purpose of a new accelerator is to find new effects in particle interactions.

This especially concerns studies of elastic hadron scattering at the LHC. It gives information about hadron interaction at large distances where perturbative QCD does not work and a new theory such as instanton or string theory, has to be developed [3].

The first measurements of the TOTEM Collaboration confirmed the non-linear behavior of the slope of the differential cross sections at a small momentum transfer [4,5], which shows a complicated picture of the hadron interaction at super high energies. The unique experiments of the TOTEM-SMS and ALFA-ATLAS Collaborations at 13 TeV gave experimental data with unprecedentedly small scattering angles and narrow Δt at small momentum transfer [6,7]. However, it is necessary to note some problems with the normalization of experimental data.

The study of the experimental data at 13 TeV obtained by the TOTEM Collaboration reveals new effects in the behavior of differential cross sections, oscillations [8], which are practically independent of the normalization of differential cross sections $d\sigma_{el}/dt$ (see below), as well as an additional anomalous term in the scattering amplitude with a large slope [9], which gives necessary contributions at small momentum transfer $-t$. It is important to study the full sets of experimental data obtained at LHC $7 \leq \sqrt{s} \leq 13$ TeV by both collaborations. For this purpose, the high energy generalized structure (HEGS) model was chosen as it has a minimum fitting parameters and gives a quantitative description of the differential cross section in a huge energy region $9 \leq \sqrt{s} \leq 13{,}000$ GeV and simultaneously in the Coulomb-hadron interference region and a large momentum transfer [10–12].

In the second section of the paper, a short analysis of experimental data on the differential cross sections of elastic proton-proton scattering is presented. In the Section 3, the new effects are analyzed in the framework of the HEGS model, taking into account experimental data of all sets of the TOTEM and ATLAS Collaborations obtained at 2.7–13 TeV. In Section 4, the results and some consequences are discussed. The conclusions are given in the Section 5.

2. Experimental Data

Now, there are 9 independent sets of elastic pp differential cross sections obtained by the ATLAS and TOTEM Collaborations at LHC energies $\sqrt{s}$ = 7–13 TeV (see Table 1), 6 of them are measured at a small t, including the Coulomb-hadron interference region (2 obtained by ATLAS and 3 by the TOTEM Collaboration). The other 3 sets are measured at large t, including the region of the dip-bump structure. At small t the values of $\sigma_{tot}(s)$ and $\rho(s, t=0)$ were obtained on the basis of experimental data. Some tension between $\sigma_{tot}(s)$ obtained by the ATLAS and TOTEM Collaborations should be noted. The difference is 3.15 mb at 7 TeV and grows to 5.6 mb at 8 TeV. Note that in [13]. some contradictions between the obtained $\sigma_{tot}(s)$ and $\rho(s, t=0)$ by the TOTEM at 7 TeV were shown. In the paper [14], some discrepancy between the slopes of the differential cross sections, measured by the TOTEM at 7 and 8 TeV, were noted.

Until recently, we had no ATLAS-AlFA data at 13 TeV. Now these data are published [7]. The tension between values of $\sigma_{tot}(s)$ increases up to 5.75 mb. In a recent paper [15], the importance of the contribution of inelastic scattering at small angles, especially in the case of determining the total cross section by the luminosity independent method. We can note the large difference in the measurements of $\sigma_{tot}(s)$ by the luminosity independent method (72 and 80 mb) by two Collaborations at the Tevatron. However, in our opinion the situation is more complicated and requires careful analysis of the new data.

The new experiment of the ATLAS-ALFA Collaboration [7] presented unique results. The position of Roman Pot situated at very large distances (2400 m) allows one to obtain new data at very small angles with small Δt. The experiment for first time gave five new experimental points in the essential Coulomb-nuclear interference region. The first experimental point begins from $-t = 0.00025$ GeV^2 with $\Delta t = 0.0001$ GeV^2. To our regret, this first point has a large error (only statistical error reaching 26 per cent). However, there are at least six-seven more points in the Coulomb Nuclear Interference (CNI) region. Three-four of them overlap the region where the TOTEM Collaboration gave own experimental points. Obviously, we can see that the ATLAS points lie systematically below the TOTEM points. Hence, they require some additional normalization. This is so, and our model description of both sets shows, in all variants of the model, the difference in the normalization is about 11–13%. As the points lie in the significant CNI region, we can check up these experimental points of ATLAS, by comparing their momentum transfer dependence with the t dependence of the contribution of the Coulomb amplitude.

Let us extract from the differential cross section of elastic scattering the term of Coulomb-nuclear interference, which is determined by the contribution of the pure Coulomb amplitude and the contribution of the pure hadron amplitude

$$\frac{d\sigma}{dt}|_{CNI} = \frac{d\sigma}{dt}|_{exper.} - \frac{d\sigma}{dt}|_{F_C^2} - \frac{d\sigma}{dt}|_{Fh^2} \qquad (1)$$

The first term proportional to the square of the Coulomb amplitude is calculated exactly and has the $1/t^2$ dependence. The second term, proportional to the square of the hadron amplitude has small t dependence in the examined t region. The result proportional to the product of Coulomb and hadron amplitude has the $1/t$ dependence. For comparison with the TOTEM data, let us take our description of all sets at 7–13 TeV without recent ATLAS data (see below) and calculate $d\sigma_{el}/dt$ at the same points of t as the ATLAS experimental data at 13 TeV. For comparison of the t dependence, let us take an artificial term that has a simple $1/t$ dependence $F_{Ch}(t) = 8\alpha_{em}/t$, where α_{em} is a fine electromagnetic structure constant. The results are presented in Table 2. Obviously, the value of Δ_{CNI} (third column of Table 2) obtained from the ATLAS data has no normal $1/t$ dependence and differs considerably from the results obtained from TOTEM artificial data (Table 2, last column). In Figure 1, the data are compared with the CNI term with hadron amplitudes, used by ATLAS (short, dashed line), and with HEGS model calculations (long-dashed line), as well as with the term which represents the true $1/t$ dependence $F_{Ch}(t) = 8\alpha_{em}/t$. We can see that the model calculations exactly reproduce the $1/t$ dependence. The points calculated with the hadron amplitude with $\sigma_{tot} = 104$ mb are much lower and give the $1/t$ dependence only for $-t > 0.0005$ GeV^2. The points obtained by using $\sigma_{tot} = 110$ mb do not givethe $1/t$ dependence for all points. It means that simple additional normalization does not improve the situation.

Table 1. Sets of $d\sigma/dt$ and χ^2_{dof} obtained in the HEGS model (k_i -additional normalization coefficient).

$\sqrt{s}$ **TeV**	n	$-t_{min}$ **(GeV^2)**	$-t_{max}$ **(GeV^2)**	$\sum \chi^2_i$	χ_{dof}	k_{norm}
7 T(1)	79	0.0699	162.1	2.19	1.12	1.01
7 A(1)	70	0.0559	86.5	1.29	1.15	1.04
8 T(2)	65	0.0488	66.3	1.07	1.16	0.93
8 A(2)	60	0.0422	55.3	0.97	1.16	1.04
8 T(3)	55	0.0361	49.7	0.96	1.16	1.04
8 T(4)	50	0.0305	47.8	1.02	1.01	0.94
13 T(5)	40	0.0207	34.2	0.92	1.11	1.06
$\sum$ AT	712	0.0007	2.4	715	1.01	$\overline{1.06}$

Table 2. $\Delta_{CNI} = d\sigma/dt_{CNI}$ mb/GeV^2.

$-t$ **(GeV^2)**	$d\sigma/dt_{ATLAS}$	$-\Delta_{CNI}$	$d\sigma/dt_{mod}$	$-\Delta_{CNI}$
0.00029	3662	-33	3291	417
0.0004	2136	33	1952	296
0.00051	1401	146	1396	229
0.00067	998	130	1034	166
0.00086	797	104	846	130
0.00112	680.1	75	731.1	98
0.00143	610.6	62	620.7	75

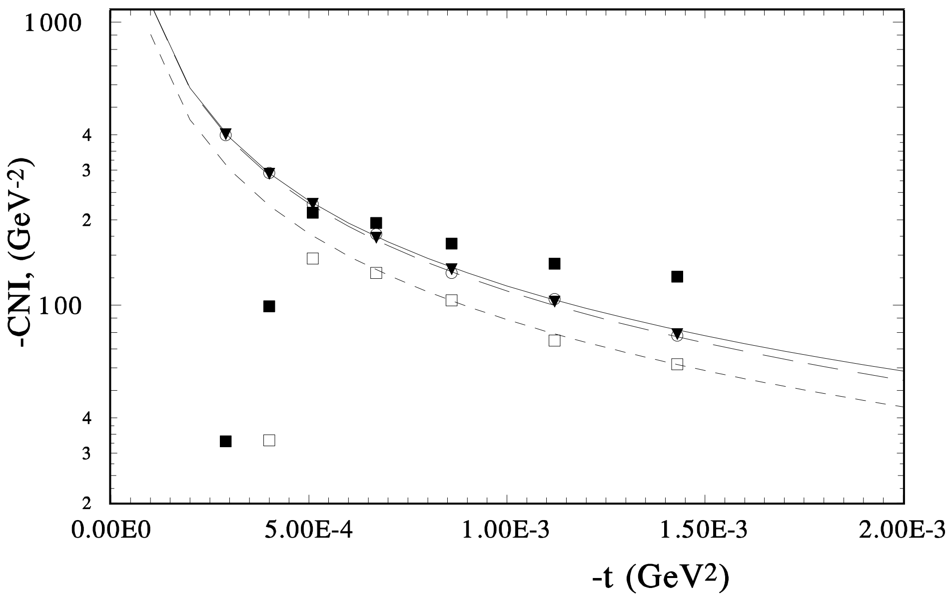

Figure 1. $\Delta_{CNI}(t)$ extracted from experimental data: open squares and full squares—with different magnitudes of $\sigma_{tot}(s) = 104$ mb and $\sigma_{tot}(s) = 110$ mb with ATLAS form of $F_h(t)$; circles—extracted from the model representation of TOTEM data; hard line—representation of the CNI-term in the form $F_{Ch}(t) = 8\alpha_{em}/t$; long dashed line—HEGS model calculations of the CNI term; short, dashed line—model calculations with ATLAS phenomenological fit of $F_h(t)$.

In Figure 2, the comparison of the TOTEM and ATLAS data at 13 TeV are presented. Obviously, the data of ATLAS above $-t = 0.0005$ GeV^2 are systematically lower than the TOTEM data. It means that additional corrections of the normalization of experimental data are required. This explains the tension between the values of $\sigma_{tot}(s)$ presented by the Collaborations. In our model fitting, we take into account only statistical errors, whereas, systematical errors are taken into account as additional correction coefficients of the normalization.

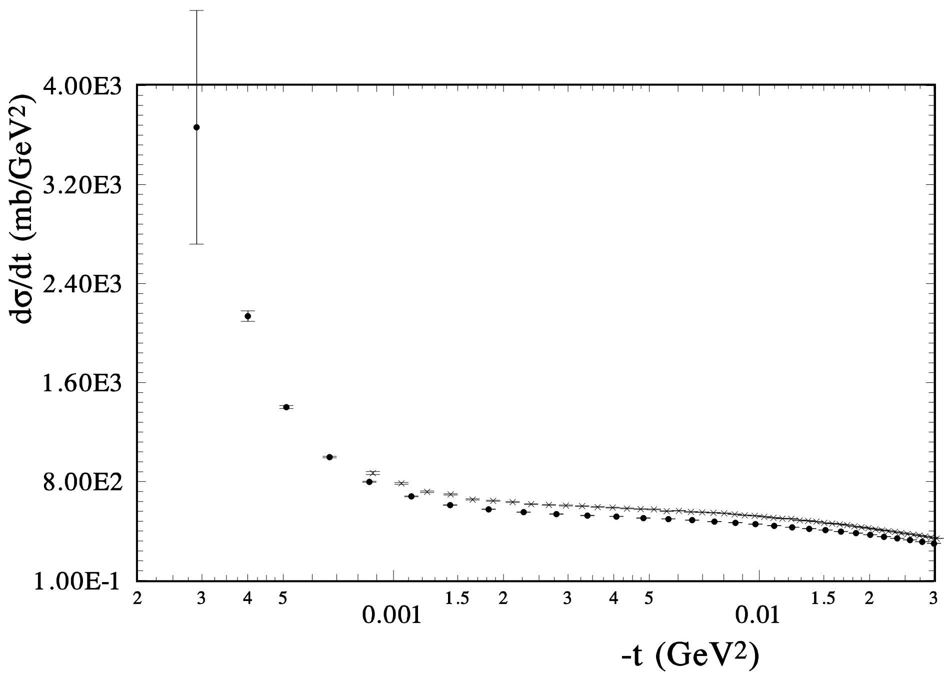

Figure 2. Comparison of experimental data on the differential cross sections at small momentum transfer of the TOTEM and ATLAS Collaboration only with statistical errors. (Full circles—ATLAS data, crosses—TOTEM data).

3. Description of All Experimental Sets at 7–13 TeV

Many different semi-phenomenological models give qualitative description of the behavior of $d\sigma_{el}/dt$ of elastic pp-scattering at $\sqrt{s} = 13$ TeV (for example [16,17]). Some examples can be found in the review [13]; hence, we do not give a deep analysis of those models. Our model was compared with other in [11] (for example, see Table VII in [11]). One of the common properties of practically all models is that they take into account statistic and systematic errors in quadrature forms and, in the most part, give only a qualitative description of the behavior of the $d\sigma_{el}/dt$ in a wide momentum transfer region. The analysis of systematic errors, for example, of the TOTEM collaboration, shows that the main uncertainty is determined by Luminosity. This affect experimental data of one set in one direction. Additional normalization reflect such a situation. This method is used by many other research groups, which deal with many different sets of experimental data, for example, in analysis of different aspects of distribution functions (PDF). In this paper, we use the high energy generalized structure (HEGS) model that is based on generalized parton distributions. The generalized parton distributions (GPDs) represent the basic properties of the hadron structure. Different properties of the hadron structure are reflected in the elastic scattering amplitude. Our form of the momentum transfer dependence of GPDs allows us to calculate the electromagnetic form factors, gravitomagnetic form factors, transition form factors, and Compton form factors. As a result, the description of various reactions is based on the same representation of the hadron structure. This allows us to use both hadron form factors (electromagnetic and gravitomagnetic) to build a high energy generalized structure model of elastic hadron-hadron scattering. The value of s and t dependence of the real part of the elastic scattering amplitude—$ReF(s,t)_B$ are determined by the complex energy $\hat{s} = s\, exp(-i\pi/2)$. Hence, the model does not introduce some special functions or assumptions for $ReF(s,t)_B$. The final elastic hadron scattering amplitude is obtained after unitarization of the Born term. So, first, we have to calculate the eikonal phase in the most favorable eikonal unitarization scheme. The eikonal phase corresponds to $F(s,t)_B$. And in the common case corresponds to the spin-dependent potential.

In our paper [8], it was shown that the new data of the TOTEM Collaboration at 13 TeV show the existence in the scattering amplitude of the oscillation term, which can be determined by the hadron potential at large distances. In the analysis of experimental data of both the sets of the TOTEM data additional normalization was used. Its values reach sufficiently large magnitudes. In this case, a very small χ^2_{dof} was obtained with considering only statistical errors and with a few number of free parameters in the scattering amplitude, which was obtained in our High Energy Generalized Structure (HEGS) model [10,11]. However, an additional normalization coefficient reaches a sufficiently large value, about 13%. It can be in a large t-region, but is very unusual for a small t Both sets of experimental data (small and large region of t) overlap in some region and, hence, affect each other's normalization. It is to be noted that the value of the normalization coefficient does not impact the magnitudes and properties of the oscillation term. We have examined many different variants of our model (including large and unity normalization coefficient), but the parameters of the oscillation term show small variations.

In the present work, all sets of the TOTEM and ATLAS data at 7–13 TeV (at first, not including recent ATLAS data at 13 TeV) are analyzed with additional normalization equal to unity and taking into account only statistical errors in experimental data.

To study the new effects in elastic scattering as a basis, we take our high energy generalized structure (HEGS) model [10,11] which quantitatively describes, with only a few parameters, the differential cross section of pp and $p\bar{p}$ from $\sqrt{s} = 9$ GeV up to 13 TeV, includes the Coulomb-hadron interference region and the high-$|t|$ region up to $|t| = 15$ GeV^2 and quantitatively well describes the energy dependence of the form of the diffraction minimum [12]. The model is simplified as much as possible in order to get the most visible impact of new members. To avoid possible problems connected with the low-energy region, we consider here only the asymptotic variant of the model, leaving only the hadron spin-flip amplitude, which has no energy dependence, and taking it in a simple exponential form with two parameters. As was made in all variants of the model, we take into account in the slope the π meson loop in the t-channel, as was proposed in [18,19] and recently studied in [20]. The total elastic amplitude in general gets five helicity contributions, but at high energy it is sufficiently to keep only spin-non-flip hadron amplitudes. In this case, one take $F(s,t) = F^{h}(s,t) + F^{\rm em}(s,t)e^{\varphi(s,t)}$ where $F^{h}(s,t)$ comes from the strong interactions, $F^{\rm em}(s,t)$ from the electromagnetic interactions and $\varphi(s,t)$ is the interference phase factor between the electromagnetic and strong interactions [21]. Note that all five spiral electromagnetic amplitudes are taken into account in the calculation of the differential cross sections. It is essential that in the model only the Born term is taken in an analytic form. After that, the eikonal phase is calculated by the Fourier-Besel method. Then using the standard eikonal representation, the full scattering amplitude is calculated numerically. The Born term of the elastic hadron amplitude at large energy can be written as a sum of two pomerons (related with two and three (cross even) gluons) and odderon contributions (cross odd—three gluon amplitude). Note that both pomeron contributions have the same positive sign, this is an essential difference from other models.

$$F(s,t)_B \;=\; \hat{s}^{\epsilon_0}\left(C_{\mathbb{P}} F_1^2(t)\; \hat{s}^{\alpha'\, t} + (C'_{\mathbb{P}} \pm i C'_{\mathbb{O}} t) A^2(t)\; \hat{s}^{\frac{\alpha' t}{4}} \right), \tag{2}$$

As seen, all terms have the same intercept $\alpha_0 = 1 + \epsilon_0 = 1.11$, and the pomeron slope is fixed at $\alpha_0^{'} = 0.24\ \mathrm{GeV}^{-2}$. With taking into account the effects of a two π-meson loop, we have $\alpha^{'} = \alpha_0^{'}(1 + x_{rt}^3 e^{-b_{sl} t Ln(s)})$ with $x_{rt} = \sqrt{4m_\pi - t}$. The model takes into account the electromagnetic $F_1(t)$ and gravitomagnetic $A(t)$ form factors, which correspond to the charge and matter distributions [22]. Both form factors are calculated as the first and second moments of the same Generalized Parton Distribution (GPDs) function. The Born scattering amplitude has three free parameters (the constants C_i) at high energy: two for the two pomeron amplitudes and one for the odderon. The real part of the hadronic elastic scattering amplitude is determined through the complexification $\hat{s} = -is$ to satisfy the dispersion relations. The oscillatory function was determined [8]

$$f_{osc}(t) = h_{osc}(1+i) J_1(\tau))/\tau;\; \tau = \pi\,(-t)/t_0\; G_{em}^2(t), \tag{3}$$

here $J_1(\tau)$ is the Bessel function of the first order and $G_{em}(t)$—the electromagnetic form factor of the proton. This form has only two additional fitting parameters and allows one to represent a wide range of possible oscillation functions.

As was found in [9], the behavior of experimental data requires an additional term to scattering amplitude in the CNI region, which is determined by the hadron interaction at large distances. In the present work, it takes a simple exponential form

$$F_d(t) = h_d(i - \rho(t)) e^{-(B_1|t| + B_2|t|^2)\log \hat{s_{13}}}\; G_{em}^2(t), \tag{4}$$

where $\rho(t)$ is determined by the main amplitude $F(s,t)$. Considering all sets of experimental data (Table 1), 715 experimental points were used in the fitting procedure with thirteen free parameters. The fitting procedure gives $\chi^2/n.d.f. = 1.06$ (remember that we used only statistical errors) with additional normalization coefficients

$$n_{A1} = 0.97, n_{T1} = 1.02, n_{T2} = 0.96, n_{A2} = 0.96, n_{T3} = 1.07,$$

$$n_{T4} = 0.96, n_{T5} = 1.09, n_{T6} = 1.09, n_{A3} = 0.96$$

If we add the experimental data of the TOTEM Collaboration at $\sqrt{s} = 2.76$ TeV [23], the number of experimental points increases to 778 and we obtain $\chi^2_{dof} = 1.07$.

The constants of the oscillatory and anomalous terms are determined with high accuracy

$$h_{osc} = 0.36 \pm 0.013; \quad h_d = 1.41 \pm 0.07\,\mathrm{GeV}^{-2}.$$

They can be compared with the same constants obtained from the analysis of the TOTEM data at 13 TeV [8,9]

$$h_{osc} = 0.16 \pm 0.02; \quad h_d = 1.7 \pm 0.01\,\mathrm{GeV}^{-2}.$$

It can be seen that additional experimental information leads to an increase in the magnitudes of the oscillation term. If such peculiarities are related with the specific properties of the TOTEM 13 TeV data only, the constants have to decrease and errors increase essentially. Note that the form and value of the oscillation are independent of additional normalization of the set of experimental data. The normalization shifts all data of one set in one direction. The oscillation term led to increasing or decreasing some parts of the model calculate differential cross sections. Hence, it is reflecting the deviations from the average position of experimental data of the set.

Now, let us add the new data of the ATLAS Collaboration at 13 TeV into our consideration. As there are some problems with the points in the CNI region, let us take them with some increasing errors (for example, twice as large or proportional to the error of the first point). The number of experimental points is 795 and $\chi^2 = 903$ is obtained. In this case, additional normalization for the ATLAS data is $n_{A3} = 1.06$, and the normalization of the TOTEM data at 13 TeV is $n_{T6} = 0.94$. This reflects the tension between these data. But the magnitudes of the corresponding constants of the new terms practically do not change. This means that such additional information does not change the determination of these peculiarities. Considering the experimental data of the TOTEM Collaboration at 2.9 TeV leads to the same result. In this case, the number of experimental points increases to 858 and $\chi^2 = 984$ is obtained. But, again the magnitudes of the constants practically do not change.

The contributions of the oscillatory term in the differential cross section of the ATLAS data at 13 TeV are presented in Figure 3a,b. In Figure 3a, the results of the statistical method of the two chosen independent selections are shown. This is the result of the procedure in which the whole examined region of momentum transfer is divided into some equal intervals, and then deviations of experimental data from some smooth curve in units of errors of experimental data were summed separately in the odd and even intervals. If some periodic structure is present in experimental data, it gives increasing sums of the contribution in the odd and even intervals in the case of coincidence of the period with the span of the interval. If the beginning of intervals is shifted by half the period, the sums will be near each other. To see the oscillations in the differential cross sections, let us determine two values—one is pure theoretical and the other with experimental data

$$R\Delta_{th} = [d\sigma/dt_{th0+osc} - d\sigma/dt_{th0}]/d\sigma/dt_{th0}, \tag{5}$$

$$R\Delta_{Exp} = [d\sigma/dt_{Exp} - d\sigma/dt_{th0}]/d\sigma/dt_{th0}.(b) \tag{6}$$

The corresponding values calculated from the fit of two sets of the ATLAS data at 13 TeV are shown in Figure 3b.

The results of the description of the differential cross sections are represented in Figure 4a,b. We can see that the diffraction minimum has a sharp form at 7 and 13 TeV, but a less pronounced at $\sqrt{s} = 2.79$ TeV.

In Figure 5, the s and t dependence of the imaginary (left) and real (right) parts of the elastic scattering amplitude obtained in the model with taking into account additional effects are represented. Note that the real part of the scattering amplitude has the first zero at small momentum transfer which changes with energy. The imaginary part of the scattering amplitude has the first zero at the essentially large momentum transfer. It determines the position of the diffraction minimum. Note that there is a crossing point on which the curves intersect. It is determined by the growth of the total cross sections and, simultaneously, the growth of the slope of the scattering amplitude.

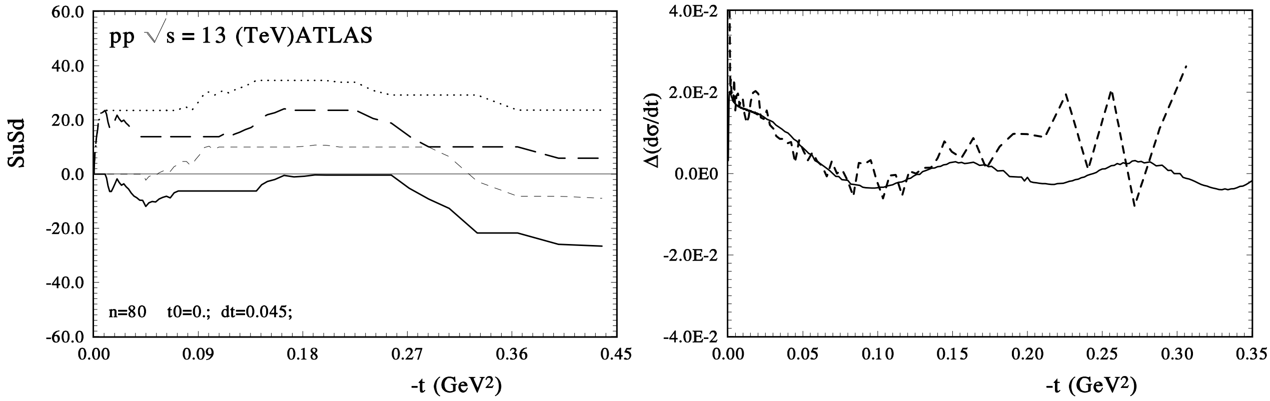

Figure 3. (**left side**) The effect of the oscillation term in the even and odd parts of the intervals of momentum transfer of ATLAS data at 13 TeV (hard and dotes lines) The same but with shifted intervals by half the period—(short, dashed lines); (**right side**) $R\Delta_{th}$ of Equation (5) (the hard line) and $R\Delta_{ex.}$ Equation (6) (the tiny line) of ATLAS data at 13 TeV.

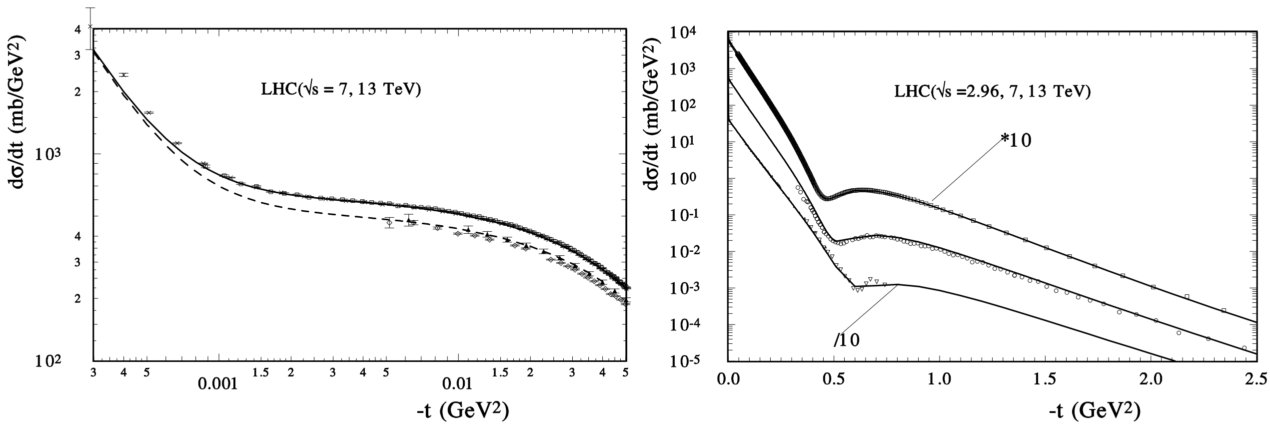

Figure 4. The $d\sigma_{el}/dt$ are calculatedin the framework of the HEGS model at 2–13 TeV (the experimental points with only statistical errors). (**right**) the full region of t; (**left**) the magnification of the region of the small momentum transfer; (the data of ATLAS ($\sqrt{s} = 13$ TeV) are drawn without an additional coefficient of the normalization.

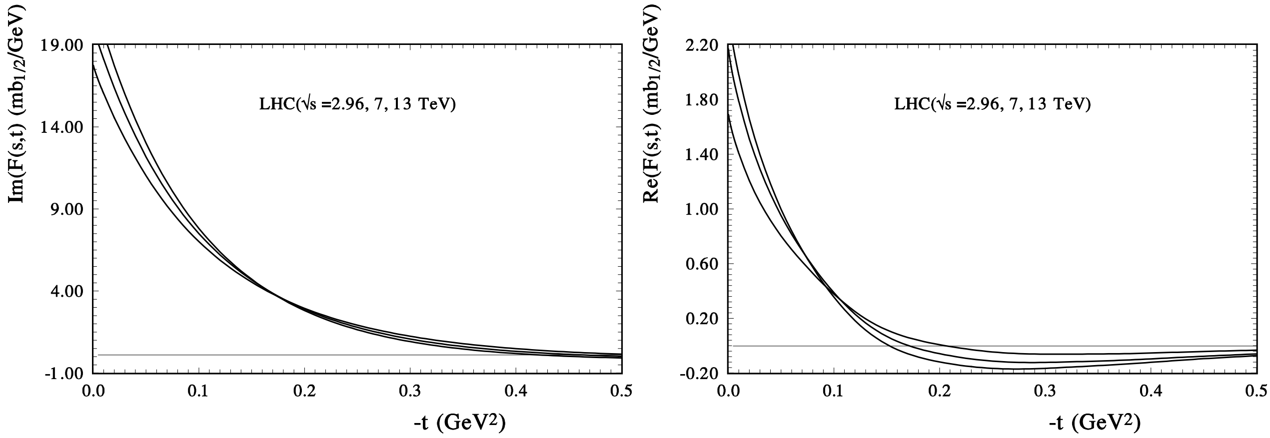

Figure 5. The s and t dependence of the imaginary (**left**) and real (**right**) parts of the elastic scattering amplitude (lines at small t correspond top down to 13, 7, 2.96 TeV).

4. Results and Discussion

Now we have some tensions between the results of the TOTEM and ATLAS Collaborations at LHC all energies. This especially concerns the extraction of magnitudes of the $\sigma_{tot}(s)$ and $\rho(s,t=0)$. New unique results of the ATLAS Collaboration do not improve the situation. The new ATLAS data present for the first time the results at very small momentum transfer. These first points and common difference between the ATLAS and TOTEM data will be crucial for the discussion of the total cross sections, rho-parameter, Odderon contributions, et cetera. Unfortunately, we found out that these points contradict the standard behavior of the electromagnetic amplitude. The analysis shows that the difference between the other points of ATLAS and TOTEM is related not with the s and t dependence of the scattering amplitude but with different normalization only, which is very important for other studies.

Examining the new peculiarity in the differential cross sections of elastic scattering at LHC energies in a wide momentum transfer on the basis of all experimental data of the TOTEM-CMS and AlFA-ATLAS Collaborations, previously found in the $d\sigma el/dt$ of the TOTEM Collaboration at 13 TeV [8,9], strongly confirm the existence of these effects. Especially, we take only statistical errors which significantly reduce the corridor of the possible s and t dependence of the scattering amplitude. The systematical errors are considered as additional normalization, which are equal for all points of the set.

The magnitude of the constants of the effects is relatively large and is determined with small errors ($h_{fd} = 1.54 \pm 0.08$ GeV^{-2} and $h_{osc} = 0.37 \pm 0.014$ GeV^{-2}), depending on the new ATLAS data at 13 TeV, and ($h_{fd} = 1.41 \pm 0.07$ GeV^{-2} and $h_{osc} = 0.36 \pm 0.013$ GeV^{-2}), and considering the new ATLAS data at 13 TeV.

The HEGS model describes at a quantitative level the new experimental data at 2–13 TeV $\chi^2_{dof} = 1.09$ without the new ATLAS data and $\chi^2_{dof} = 1.16$ with considering only statistical errors (see Figure 5). Such a description can be obtained only considering the new peculiarities of the elastic differential cross sections.

The new phenomena are determined by hadron interactions at large distances. The corresponding hadron potential has no simple exponential behavior. Our calculations [24] show that it has a modified Gaussian form with probably a cut at large distances $V(r) = hExp[-Br^2]/(R_0 + r)$. This may be due to glueball states of the gluon. In such a form, the gluon can be distributed at large distances above the confinement level.

The new effects can impact the determination of values of the total cross sections, the ratio of the elastic to the total cross sections, and $\rho(s,t)$, the ratio of the real to imaginary part of the elastic scattering amplitude. As a result, we have obtained the values of $\sigma_{tot}(s)$ and $\rho(s)$ represented in Table 3.

It is very likely that such effects exist also in experimental data at essentially lower energies [25], but, maybe, they have a more complicated form (with two different periods, for example).

Table 3. The $\sigma_{tot}(s)$ and $\rho(s)$ obtained in the HEGSh model.

$\sqrt{s}$ (GeV)	$\sigma_{tot-ATLAS}$	$\sigma_{tot-TOTEM}$	$\sigma_{tot-model}$	$\rho_{tot-ATLAS}$	$\rho_{tot-TOTEM}$	$\rho_{tot-model}$
7.	95.35 ± 2	98.5 ± 2.9	98.8 ± 1.4		0.145 ± 0.09	0.117 ± 0.03
8.	102.9 ± 2.3	101.7 ± 2.9	100.7 ± 1.4		0.12 ± 0.03	0.118 ± 0.04
13.	104.7 ± 1.1	110.6 ± 0.6	108.1 ± 1.4	0.098 ± 0.011	0.1 ± 0.01	0.119 ± 0.04

5. Conclusions

Our critical analysis of the new experimental data obtained by the ATLAS Collaboration group at 13 TeV shows that the first experimental points contradict the behavior of the electromagnetic amplitude at small momentum transfer.

To remove such contradiction, it is necessary to take these points with large errors. The problem of tension between the ATLAS and TOTEM Collaborations data lies more part in different normalisation.

The analysis is based on all sets of experimental data of the elastic differential cross section in a wide region of momentum transfer confirms the existence of the new effects discovered on the basis of experimental data at 13 TeV [8,9] and associated with the specific properties of the hadron potential at large distances.

As a result, we have shown that the new peculiarities in the scattering amplitude are confirmed by all LHC data, and are not artificial or instrumental effects of one experiment. The existence of such peculiarities is important for our understanding of the nucleon interaction at large distances. Hence, it opens up a new direction in the study of hadron structure and interaction at super high energies and large distances.

Funding: This research received no external funding.

Conflicts of Interest: The author declares no conflict of interest.

References

1. Uzikov, Y.N.; Temerbayev, A.A. Null-test signal for T-invariance violationin pd scattering. *Phys. Rev. C* **2015**, *92*, 014002–014009.
2. Sacharov, A.D. Violation of CP Invariance, C asymmetry, and baryon asymmetry of the universe. *JETP Lett.* **1967**, *5*, 24–27.
3. Dorokhov, A.E.; Kochelev, N.I.; Zubov, Y.A. Proton spin within nonperturbative QCD. *Int. J. Mod. Phys. A* **1993**, *8*, 603–651. [CrossRef]
4. Antchev, G. TOTEM Collaboration, Measurement of Elastic pp Scattering at $\sqrt{s} = 8$ TeV in the Coulomb-Nuclear Interference Region—Determination of the ρ-Parameter and the Total Cross-Section. *Eur. Phys. J. C* **2016**, *76*, 661.
5. Antchev, G.; Aspell, P.; Atanassov, I.; Avati, V.; Baechler, J.; Barrera, C.B.; Berardi, V.; Berretti, M.; Bossini, E.; Bottigli, U.; et al. Evidence for non-exponential elastic proton–proton differential cross-section at low $|t|$ and $\sqrt{s} = 8$ TeV by TOTEM. *Nucl. Phys. B* **2015**, *899*, 527–546. [CrossRef]
6. Antchev, G.; Aspell, P.; Atanassov, I.; Avati, V.; Baechler, J.; Barrera, C.B.; Berardi, V.; Berretti, M.; Bossini, E.; Bottigli, U.; et al. Elastic differential cross-section measurement at $\sqrt{s} = 13$ TeV by TOTEM. *Eur. Phys. J. C* **2019**, *79*, 861.
7. ATLAS Collaboration. Measurement of the total cross section and ρ-parameter from elastic scattering in pp collisions at $\sqrt{s} = 13$ TeV with the ATLAS detector. *arXiv* **2022**, arXiv:2207.12246.
8. Selyugin, O.V. New feature in the differential cross sections at 13 TeV be measured at the LHC. *Phys. Lett. B* **2019**, *797*, 134870–134873. [CrossRef]
9. Selyugin, O.V. Anomaly in the differential cross sections at 13 TeV. *Mod. Phys. Lett. A* **2021**, *36*, 2150148. [CrossRef]
10. Selyugin O.V. GPDs of the nucleons and elastic scattering at high energies. *Eur. Phys. J. C* **2012**, *72*, 2073–2086.
11. Selyugin, O.V. Nucleon structure and the high energy interactions. *Phys. Rev. D* **2015**, *91*, 113003; Erratum in *Phys. Rev. D* **2015**, *92*, 099901. [CrossRef]
12. Selyugin, O.V. The energy dependence of the diffraction minimum in the elastic scattering and new LHC data. *Nucl. Phys. A* **2017**, *959*, 116. [CrossRef]
13. Pancheri, G.; Yogendra Srivastava, N. Introduction to the physics of the total cross-section at LHC: A Review of Data and Models. *arXiv* **2016**, arXiv:1610.10038.
14. Donnachie, A.; Landshoff, P.V. Lack of evidence for an odderon at small t. *arXiv* **2022**, arXiv:2203.00290.
15. Grafstrom, P. Comments on low mass dissociation at the LHC in the context of the discrepancy between the ATLAS and TOTEM measurements of σ_{tot}. *arXiv* **2022**, arXiv:2209.01058.
16. Petrov, V. Diffractive Scattering: Problems in Theory and Praxis. *arXiv* **2017**, arXiv:1711.00226.
17. Ferreira, E.; Kohara, A.K.; Sesma, J. Exact treatment of dispersion relations in pp and pp elastic scattering. *Phys. Rev. C* **2018**, *97*, 014003. [CrossRef]
18. Anselm, A.; Gribov, V. Zero pion mass limit in interactions at very high-energies. *Phys. Lett. B* **1972**, *40*, 487–493. [CrossRef]
19. Cohen-Tannoudji, G.; Ilyin, V.V.; Jenkovszky, L.L. A model for the pomeron trajectory. *Lett. Nuovo Cim.* **1972**, *5*, 957–962. [CrossRef]
20. Khoze, V.A.; Martin, A.D.; Ryskin, M.G. t dependence of the slope of the high energy elastic pp cross section. *J. Phys. G* **2015**, *42*, 025003. [CrossRef]
21. Selyugin, O.V. Coulomb Hadron Phase Factor And Spin Phenomena In A Wide Region Of Transfer Momenta. *Phys. Rev. D* **1999**, *60*, 074028. [CrossRef]
22. Selyugin, O.V. Models of parton distributions and the description of form factors of nucleon. *Phys. Rev. D* **2014**, *89*, 093007. [CrossRef]
23. Antchev, G.; Aspell, P.; Atanassov, I.; Avati, V. Elastic differential cross-section $d\sigma/dt$ at $\sqrt{s} = 2.76$ TeV and implications on the existence of a colourless 3-gluon bound state. *Eur. Phys. J. C* **2020**, *80*, 91. [CrossRef]

24. Selyugin, O.V. Hadron interaction at large distances and new peculiarities of the differential cross sections, at LHC energies. In Proceedings of the International Conference on Quantum Field Theory, High-Energy Physics, and Cosmology, JINR, Dubna, Russia, 18–21 July 2022.
25. Selyugin, O.V.; Cudell, J.-R. Long-range potential and the fine structure of the diffraction peak. *AIP Conf. Proc.* **2011**, *1350*, 115–118.